Xenopus laevis Actin-depolymerizing Factor/Cofilin: A Phosphorylation-regulated Protein Essential for Development

Hiroshi Abe,* Takashi Obinata,* Laurie S. Minamide,‡ and James R. Bamburg‡

*Department of Biology, Chiba University, Chiba 263, Japan; and ‡Department of Biochemistry and Molecular Biology and Program in Neuronal Growth and Development, Colorado State University, Fort Collins, Colorado 80523

Abstract. Two cDNAs, isolated from a *Xenopus laevis* embryonic library, encode proteins of 168 amino acids, both of which are 77% identical to chick cofilin and 66% identical to chick actin-depolymerizing factor (ADF), two structurally and functionally related proteins. These *Xenopus* ADF/cofilins (XACs) differ from each other in 12 residues spread throughout the sequence but do not differ in charge. Purified GST-fusion proteins have pH-dependent actin-depolymerizing and F-actin–binding activities similar to chick ADF and cofilin. Similarities in the developmental and tissue specific expression, embryonic localization, and in the cDNA sequences of the noncoding regions, suggest that the two XACs arise from allelic variants of the pseudotetraploid *X. laevis*.

Immunofluorescence localization of XAC in oocyte sections with an XAC-specific monoclonal antibody shows it to be diffuse in the cortical cytoplasm. After fertilization, increased immunostaining is observed in two regions: along the membrane, particularly that of the vegetal hemisphere, and at the interface between the cortical and animal hemisphere cytoplasm. The cleavage furrow and the mid-body structure are stained at the end of first cleavage. Neuroectoderm derived tissues, notochord, somites, and epidermis stain heavily either continuously or transiently from stages 18–34. A phosphorylated form of XAC (pXAC) was identified by 2D Western blotting, and it is the only species found in oocytes. Dephosphorylation of >60% of the pXAC occurs within 30 min after fertilization. Injection of one blastomere at the 2 cell stage, either with constitutively active XAC or with an XAC inhibitory antibody, blocked cleavage of only the injected blastomere in a concentration-dependent manner without inhibiting nuclear division. The cleavage furrow of eggs injected with constitutively active XAC completely regressed. Blastomeres injected with neutralized antibody developed normally. These results suggest that XAC is necessary for cytokinesis and that its activity must be properly regulated for cleavage to occur.

THE actin cytoskeleton is an essential component for cell motility, establishment of cell polarity, and maintenance of cell shape (for review see Stossel, 1993). These are critical events for organismal development and the functioning of the differentiated state. Many different types of actin-binding proteins are involved in the organization of the actin cytoskeleton and its dynamic reorganization in response to environmental cues (Pollard and Cooper, 1986; Bamburg and Bernstein, 1991). Among these are the ubiquitous F-actin binding/severing and monomer sequestering proteins of the actin depolymerizing factor (ADF)[1]/cofilin family (for review see Sun et al., 1995). At least one member of this protein family has been found in all eukaryotic organisms examined (animals, protists, and plants). Both ADF and cofilin genes are expressed in mammals, and often one or the other will dominate in a particular cell type. These proteins are enriched in neuronal growth cones and in ruffling membranes, regions of high actin assembly dynamics (Bamburg and Bray, 1987; Yonezawa et al., 1987), and in the cleavage furrow of cells undergoing cytokinesis (Nagaoka et al., 1995). Avian and mammalian ADF/cofilins are regulated by phosphorylation (Ohta et al., 1989; Morgan et al., 1993; Agnew et al., 1995; Moriyama et al., 1996), but this type of regulation may extend to other vertebrates and invertebrates as well.

The ADF/cofilin protein in *Saccharomyces cerevisiae* is an essential component of the cortical actin cytoskeleton (Moon et al., 1993; Iida et al., 1993; Mulholland et al., 1994). The ability of either mammalian ADF or mammalian cofilin to rescue yeast deficient in cofilin confirms that these proteins have a high degree of functional equivalency (Moon et al., 1993; Iida et al., 1993). Functional mutations in the ADF/cofilin protein in *Drosophila* (Edwards, 1994) are also lethal (Gunsalus et al., 1995). In

Address all correspondence to James R. Bamburg, Department of Biochemistry and Molecular Biology, Fort Collins, CO 80523. Tel.: (970) 491-0425. Fax: (970) 491-0494. e-mail: jbamburg@vines.colostate.edu

1. *Abbreviations used in this paper.* ADF, actin depolymerizing factor; GST, glutathione-*S*-transferase; KLH, keyhole lympet hemocyanin; NBT, nitroblue tetrazolium chloride; NEpHGE, nonequilibrium pH gradient gel electrophoresis; 3'UTR, 3' untranslated region of mRNA; XAC, *Xenopus* ADF/cofilin; pXAC, phosphorylated form of XAC.

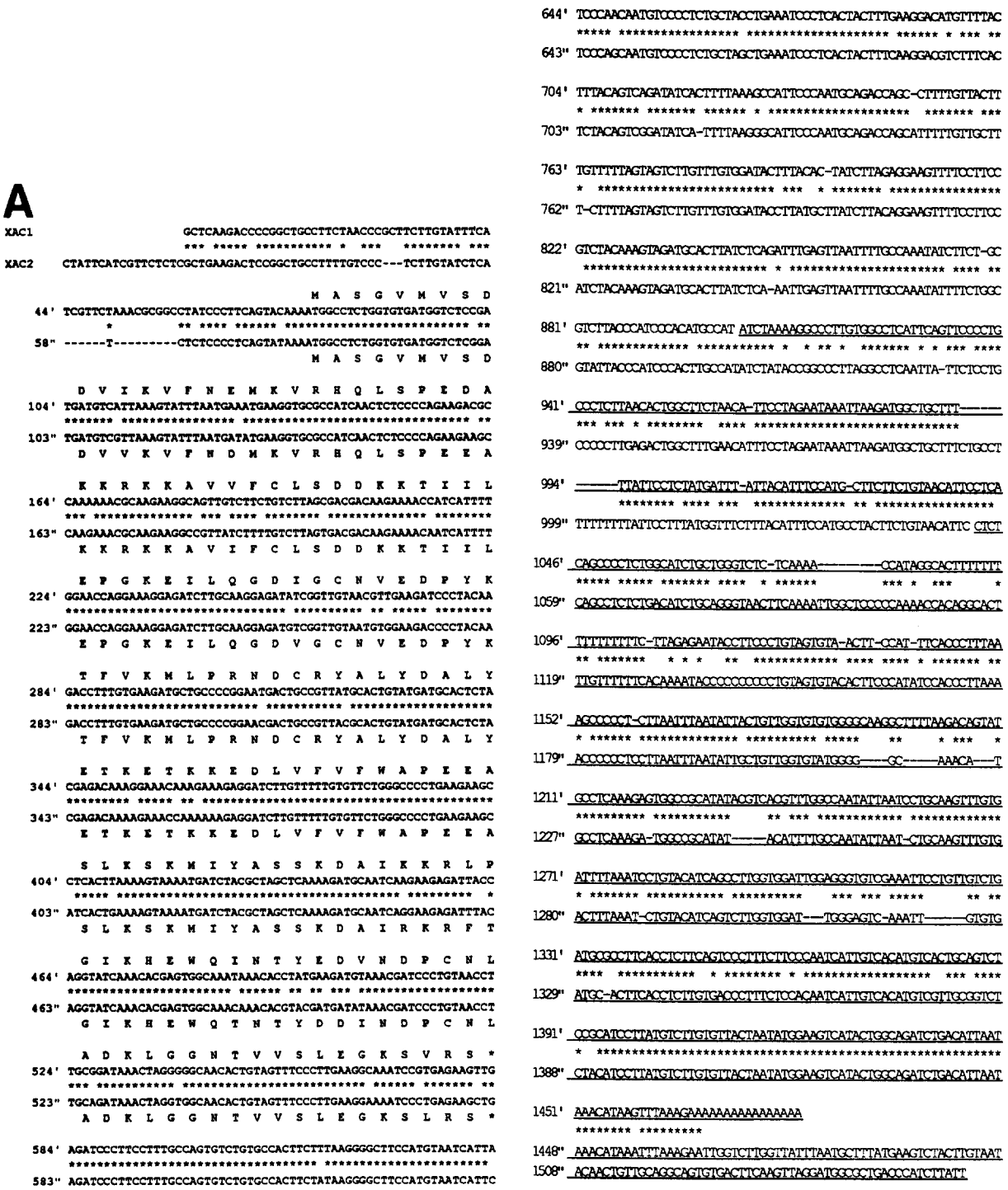

Figure 1. (*A*) Sequence of XAC cDNAs and the encoded proteins. Regions at the 3′-ends used for the probes for Southern and Northern blots are underlined. These sequence data are available from GenBank/EMBL/DDBJ under accession numbers U26270 (XAC1) and U26269 (XAC2). (*B*) Comparison of the XAC1 and XAC2 protein sequences to those of chicken cofilin and ADF. The regulatory phosphorylation site (▼) and the region used for preparation of isoform specific antibodies (*underline*) are shown.

Caenorhabditis elegans, mutations of the ADF/cofilin gene (unc-60) lead to an uncoordinated lethal mutation arising from abnormal actin assembly into contractile units in developing body wall muscle (McKim et al., 1994). Thus, ADF/cofilins play essential roles in the development of lower eukaryotic organisms. However, their expression, activity, and distribution in early vertebrate development have not been explored.

To study the role of these proteins during vertebrate development, we selected *X. laevis*, a rapidly developing, easily manipulated organism in which all developmental stages are readily observable. As a first step in these stud-

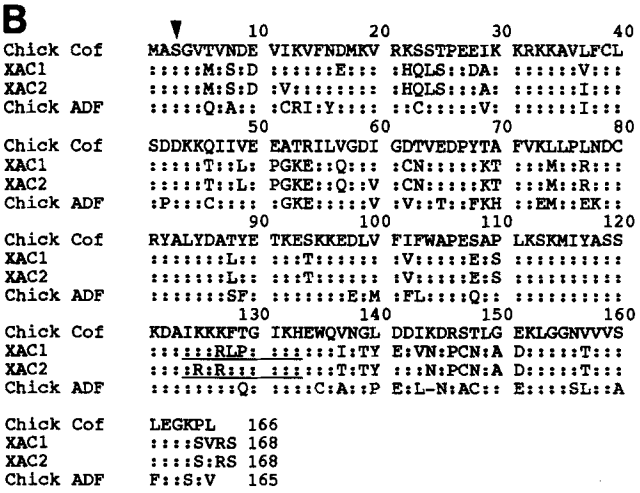

ies, we describe the cloning and characterization of two ADF/cofilin related proteins, probably allelic variants, which are maternally expressed and developmentally regulated by phosphorylation. By microinjecting embryos with an active, nonphosphorylatable form of the protein or an inhibitory antibody to the protein, we show that progression through cytokinesis requires the proper level of active *Xenopus* ADF/cofilin.

Materials and Methods

Cloning of Xenopus ADF/Cofilin cDNAs

A stage 30 *Xenopus* cDNA library in γZAP (Clontech, Palo Alto, CA) was screened with full-length cDNA probes to chicken ADF and chicken cofilin (Abe et al., 1990; Adams et al., 1990). Eight clones identified with the ADF cDNA probe and seven clones identified with the cofilin probe were selected for further study. The inserts were transferred to pBluescript SK$^-$ by in vivo excision, restriction mapped, and partially sequenced. They fell into two groups designated *Xenopus* ADF/cofilin1 (XAC1) and XAC2. One cDNA from each group was sequenced completely (from the full-length cDNA and partial deletion mutants) by the dideoxynucleotide method (Sanger et al., 1977).

Southern and Northern Blotting

Genomic DNA was prepared from adult *Xenopus* liver by the method of Blin and Stafford (1976). Single and double restriction endonuclease digestions were performed before electrophoresis, transfer to nitrocellulose, and hybridization to probes specific for each XAC cDNA. Northern blotting was performed on total RNA prepared from staged embryos and adult tissues by the procedure of Chomczynski and Sacchi (1987). DNA probes for both Southern and Northern blotting were prepared from deletion mutants which contained only part of the 3′UTR of each cDNA (906-1482 for XAC1, No. 1055-1507 for XAC2) (see Fig. 1). Some Northern blots were probed using the DNA coding region of XAC1 prepared from the NcoI to BglII site in pBluescript as described below.

Preparation of Expression Vectors

The XAC1 and XAC2 cDNAs in pBluescript SK$^-$ were amplified by PCR using a 5′ primer (5′-ACCATGGCCTCTGGTGTG-3′) which inserted an NcoI site at the initiating codon and a 3′ primer (5′-GAGATCTCAACTTCTCACGGATTT-3′) which inserted a BglII site at the 3′ end. These PCR products were cloned directly into the EcoRV site of pBluescript II KS$^+$. The cDNAs were removed by digestion with NcoI and BglII for insertion into the NcoI/SmaI sites of a modified pGEX vector (Pharmacia LKB Biotechnology, Piscataway, NJ) by blunt end ligation to produce glutathione-*S*-transferase fusion proteins. The modified pGEX vector containing an NcoI site was prepared by linearizing pGEX with BamHI, blunt ending the fragments with Klenow polymerase, inserting chicken cofilin cDNA, selecting for correct orientation, and removing the cofilin cDNA with NcoI and SmaI.

Expression and Purification of Recombinant Proteins

The pGEX expression plasmids containing XAC1 and XAC2 were transformed into XL1-Blue and recombinant protein expressed using standard procedures (Studier et al., 1990; Pharmacia, Piscataway, NJ). The GST-fusion proteins were purified on a glutathione column according to the manufacturer's directions (Pharmacia), dialyzed in PBS, and stored at −70°C after freezing in liquid nitrogen. For actin-binding studies, GST-fusion proteins were cleaved with thrombin (Sigma Chem. Co., St. Louis, MO; 12 U/mg GST-fusion protein). Concentrations of proteins were determined by a solid-phase dye-binding assay (Minamide and Bamburg, 1990).

Antibody Production

Polyclonal antibody was raised in rabbits against either GST-XAC1 or each of two synthetic decapeptides, IKKRLPGIKH from XAC1 and IRKRFTGIKH from XAC2, each containing a three amino acid NH_2-terminal linker (CGG) conjugated to keyhole lympet hemocyanin (KLH) (Macromolecular Resources, Fort Collins, CO). KLH (1 mg/200 μl serum) was used to remove cross-reactive antibodies from the serum to the peptide conjugates. Antibodies to the peptides were affinity purified on a column of peptide coupled to Sulfolink resin (Pierce Chem. Co., Rockford, IL).

Monoclonal antibodies were prepared from rats inoculated with either the GST-XAC1 or GST-XAC2 fusion proteins. Rat lymph node cells were fused with the mouse myeloma cell line P3U1 and were selected by standard cloning methods (Furuse et al., 1993; Kohler et al., 1980). Two IgG-producing clones (1A11 and 2F10) were isolated and expanded in RPMI medium (Life Technologies, Inc., Gaithersburg, MD) containing 15% FBS. Growth of the 2F10 line required supplementation with 1% BM-condimed H1 (Boehringer Mannheim, Indianapolis, IN). Hybridoma supernatant was stored at 4°C or frozen at −70°C for future use.

An anti-actin polyclonal antibody was obtained as a gift from Dr. I. Yahara, Tokyo Metropolitan Institute of Medical Science (Iida and Yahara, 1986). Its specificity against *Xenopus* actin was confirmed by Western blots of an egg protein extract.

Activity Assays for Recombinant ADF/Cofilin

The DNase I inhibition assay (Harris et al., 1982) was used to quantify the depolymerization of F-actin by the GST-XAC1 and GST-XAC2 fusion proteins. The DNase I was calibrated with muscle G-actin. The pH-dependent binding of XAC1 and XAC2 to F-actin was measured at pH 6.8 and 8.0 by sedimentation and SDS-PAGE (Hayden et al., 1993).

Polyacrylamide Gel Electrophoresis and Western Blotting

SDS-PAGE on 15% polyacrylamide isocratic mini-slab gels, and two dimensional gel electrophoresis on mini-slab gels was performed as described previously (Bamburg et al., 1991). Nonequilibrium pH gradient electrophoresis (NEpHGE) (O'Farrell et al., 1977) was used in the first dimension.

Electroblotting onto polyvinylidene difluoride (PVDF) membrane (Immobilon P; Millipore, Bedford, MA), blocking and immunostaining were performed as previously described (Bamburg et al., 1991). Primary antibody was the hybridoma supernatant (1A11 or 2F10) to XAC or purified antibodies to the XAC1 or XAC2 peptides. Alkaline phosphatase–conjugated goat anti-rat IgG or goat anti-rabbit IgG (Life Technologies, Inc.) was the secondary antibody. Chemiluminescent detection with Lumiphos (Boehringer Mannheim) was followed by staining with nitroblue tetrazolium chloride (NBT) and 5-bromo-4-chloro-3-indolylphosphate *p*-toluidine salt (BCIP) (Life Technologies, Inc.). Spot densities from film or blots were obtained from scans in transmittance or reflectance modes, respectively, using a Microscan 2000 image analysis system (Technology Resources Inc., Knoxville, TN).

Preparation of Embryos and Embryo Extracts

X. laevis embryos (wild type or albino) were obtained by fertilizing eggs from females induced with human chorionic gonadotropin, dejellying, and

culturing in Steinberg's solution at room temperature (Kay and Peng, 1991). Staging was according to Nieuwkoop and Faber (1967).

Protein extracts were prepared from eggs, embryos, and adult tissues by lysing in 2% SDS, 10 mM Tris, pH 7.5, 20 mM NaF, 2 mM EGTA, 10 mM DTT (25 μl per embryo), heating the lysate for 3 min in a boiling water bath, and precipitating the proteins with chloroform/methanol (Wessel and Flügge, 1984). Proteins were redissolved in either SDS-sample preparation buffer (Laemmli, 1970) for SDS-PAGE or in urea lysis buffer (O'Farrell, 1975) for NEpHGE.

Fixation of Embryos

For in situ hybridization or immunocytochemistry *Xenopus* embryos were fixed in 0.1 M MOPS, pH 7.4, 2 mM EGTA, 1 mM $MgSO_4$, 3.7% formaldehyde for 1 h at room temperature and then in 70% ethanol (3× 30 min) (Harland, 1991). The same fixative containing 2% trichloroacetic acid was used to fix antibody injected embryos for 2 h before ethanol dehydration. For in situ hybridization embryos were stored at this stage. For immunocytochemistry, embryos were transferred to 100% ethanol and stored. All fixation, labeling, and washing steps were carried out while the embryos were gently tumbling on a rotating mixer.

In Situ Hybridization

For in situ hybridization, digoxigenin-labeled single stranded RNA probes were prepared using the DIG RNA Labeling Kit (Boehringer Mannheim) after the manufacturer's procedures. The XAC1 and XAC2 cDNAs cloned into pBluescript KS^- were linearized either with EcoR1 and transcribed with T7 polymerase to generate the sense probe or with HindIII and transcribed with T3 polymerase (Toyobo, Japan) to generate the antisense probe.

In situ hybridization was done according to Harland (1991) except prehybridization was carried out with 5× SSPE (0.75 M NaCl, 0.2 M NaH_2PO_4, 5.5 mM EDTA, pH 7.4) substituted for the 5× SSC, and 20% goat serum was used as a blocking agent. The alkaline phosphatase conjugated anti-digoxigenin antibody (Boehringer Mannheim, Indianapolis, IN) was developed with NBT/BCIP as the chromogenic substrate for 1–3 h. Embryos were transferred to 100% ethanol to stop the development and cleared in a 1:2 mixture of benzyl alcohol and benzyl benzoate for photography.

Whole Mount Immunocytochemistry

Fixed albino embryos were put back into 70% ethanol for 1 h, PBS for 1 h, and 20% goat serum in PBS for 1 h. Embryos were incubated in 2F10 hybridoma supernatant at 4°C overnight, rinsed and washed in PBS containing 0.3% Tween-20 (3× 1 h). Incubation in secondary antibody (alkaline phosphatase–conjugated goat anti-rat IgG) diluted into 20% goat serum in PBS was done at 4°C overnight. Embryos were then rinsed and washed in PBS containing 0.3% Tween-20 (3× 1 h) and incubated in NBT/BCIP (as for in situ hybridization) for 10–30 min as color developed. The reaction was stopped by transferring the embryos to 70% ethanol and then to 100% ethanol. Embryos were cleared in a 1:2 mixture of benzyl alcohol and benzyl benzoate for photography.

Sectioning and Immunofluorescence

Fixed wild-type embryos in 100% ethanol were embedded in paraffin and 5- or 6-μm-thick sections cut and mounted on ovalbumin-coated slides. After blocking with 20% goat serum in PBS for 1 h, sections were incubated with 2F10 hybridoma supernatant, rabbit antiserum to XAC1, or rabbit antiserum to actin (Iida and Yahara, 1986) for 1 h at room temperature, and then with an appropriate fluorescein-labeled secondary antibody. After each step the sections were rinsed and washed in PBS containing 0.3% Tween-20 (2× 30 min). Sections were mounted in PBS containing 1 mg/ml *p*-ethylenediamine and 90% glycerol (Johnson and de C. Nogueira Araujo, 1981) for fluorescence microscopy.

Microscopy

Stained albino embryos and microinjected embryos were examined using overhead illumination on a Zeiss Stemi 200-C dissection microscope and photographed with Fujichrome film (ASA100). Phase contrast and immunofluorescence micrographs (8-s exposures) of *Xenopus* embryo sections were obtained on Kodak Tri-X film (ASA 400) using a 16× fluorescence objective on a Zeiss Universal epifluorescence microscope. Photography and printing of immunofluorescence micrographs were matched to those of preimmune (or nonimmune) controls (for polyclonal antiserum) or secondary antibody alone (for monoclonal antibodies). Since printing time was adjusted so that the controls gave black images, no control images are shown.

Microinjection Studies

For microinjection into fertilized eggs or one blastomere of two cell embryos, the GST-XAC1 was concentrated on a Centricon-30 (Amicon Corp., Danvers, MA) to 10 mg/ml and dialyzed against the injection buffer (2 mM Hepes, pH 7.5, 88 mM NaCl, 1 mM KCl and 2 mM $MgCl_2$). The IgG fraction of the GST-XAC rabbit antiserum was purified on protein G–agarose, dialyzed in phosphate buffered saline, freeze dried, dissolved in water at 25 mg/ml and dialyzed against injection buffer. It was diluted to 7–15 mg/ml for microinjection. A neutralized IgG fraction was prepared by mixing one part of the IgG (25 mg/ml) with four parts of the GST-XAC (10 mg/ml), freeze drying, and dissolving in water to a final IgG concentration of 10 mg/ml. All samples were centrifuged at 12,000 *g* for 2 min to remove particulates before injection. Injection volumes delivered by each

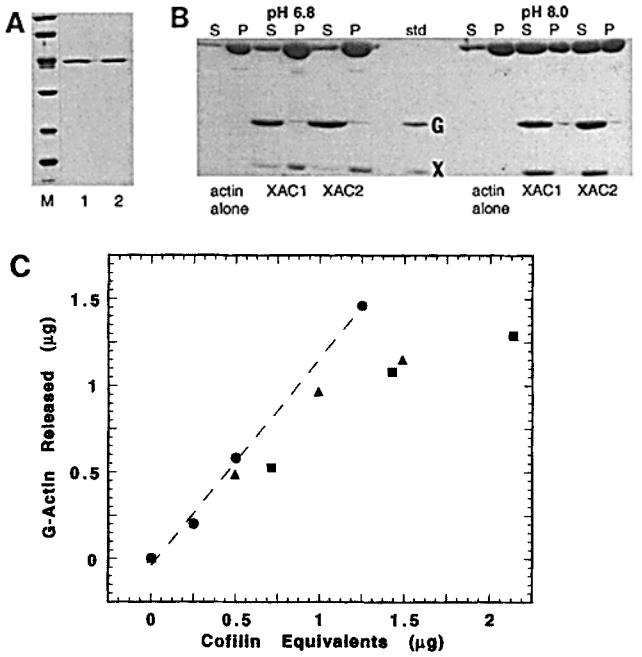

Figure 2. (*A*) Purified GST-XAC fusion proteins from glutathione column. Lanes: (*M*) Molecular mass markers (116, 97, 45, 31, 21, 14 kD); (*1*) 2 μg GST-XAC1; (*2*) 2 μg GST-XAC2. (*B*) pH-dependent F-actin binding of XAC1 and XAC2. Approximately 4 μM XAC was mixed with 5 μM G-actin (final concentrations) in 30 mM Pipes, pH 6.8, or 30 mM Tris, pH 8.0 each containing 1 mM DTT and 0.2 mM ATP. KCl and $MgCl_2$ were added to give 0.1 M and 2 mM final concentrations, respectively, in 50 μl final volume. After 60 min the samples were centrifuged at 170,000 *g* for 30 min. The supernate was removed, mixed, and a 40-μl aliquot removed for analysis by SDS-PAGE. The pellet was washed once with the buffer and salt mixture, and then solubilized in SDS sample preparation buffer. Volumes loaded on the gel represent an identical fraction of the supernatant (*S*) and pellet (*P*) protein. Standard is thrombin-cleaved GST-XAC1: *G*, glutathione-*S*-transferase; *X*, XAC. (*C*) Depolymerization of F-actin (3 μg) by GST-XAC1 (■) and GST-XAC2 (▲) were compared to recombinant chick cofilin (●) by measuring the amount of G-actin released using the DNase I inhibition assay. The DNase I was calibrated using muscle G-actin.

pipette from a pressure injector were calibrated by measuring the volume of an aqueous drop delivered into mineral oil. Control injections with nonimmune IgG (10 mg/ml) were also done. Development of embryos, along with untreated controls, were followed for the times described in text.

Results

Two Embryonic cDNAs Encode Xenopus ADF/Cofilins

Restriction mapping and partial sequencing of the 15 clones selected from a *Xenopus* stage 30 cDNA library screened with chicken ADF and cofilin cDNAs showed that the clones fell into two groups. One member of each group was sequenced completely. The two cDNAs (Fig. 1 *A*), named XAC1 and XAC2 for *Xenopus* ADF/cofilin, are 85% homologous with each other and are over 93% homologous within the open reading frame. Each cDNA is 53–54% and 51% homologous to the cDNAs encoding chicken cofilin and ADF, respectively. Within the open reading frame the homologies of both XAC cDNAs are 69 and 65% to cDNAs encoding chick cofilin and ADF, respectively. The proteins encoded by the open reading frame of XAC1 and XAC2 (Fig. 1) are 93% identical, differing from each other in only 12 out of the 168 residues. The only nonconservative differences are pro/thr and ile/thr at residues 129 and 137, respectively. Neither gives rise to any charge difference between the species. Both XAC proteins are 77% identical to chicken cofilin and 66% identical to chicken ADF (Fig. 1 *B*). The molar extinction coefficient at 280 nm of 19,420 LM^{-1} cm^{-1}, calculated from the deduced amino acid sequences (Gill and von Hippel, 1989), is identical for the two proteins.

Each cDNA was expressed in *E. coli* as a fusion protein with glutathione-*S*-transferase (GST) and purified in a single step on a glutathione column (Fig. 2 *A*). Because the GST-XAC chimeric proteins have identical mobility on SDS-PAGE with actin, we first cleaved the GST chimeras with thrombin (Fig. 2 *B*) to measure binding of the expressed XACs to F-actin. At pH 6.8, both XAC1 and XAC2 primarily bound to and sedimented with F-actin, while at pH 8.0 both proteins primarily were in the supernatant along with an increased amount of unpolymerized actin. The GST released by thrombin remained in the su-

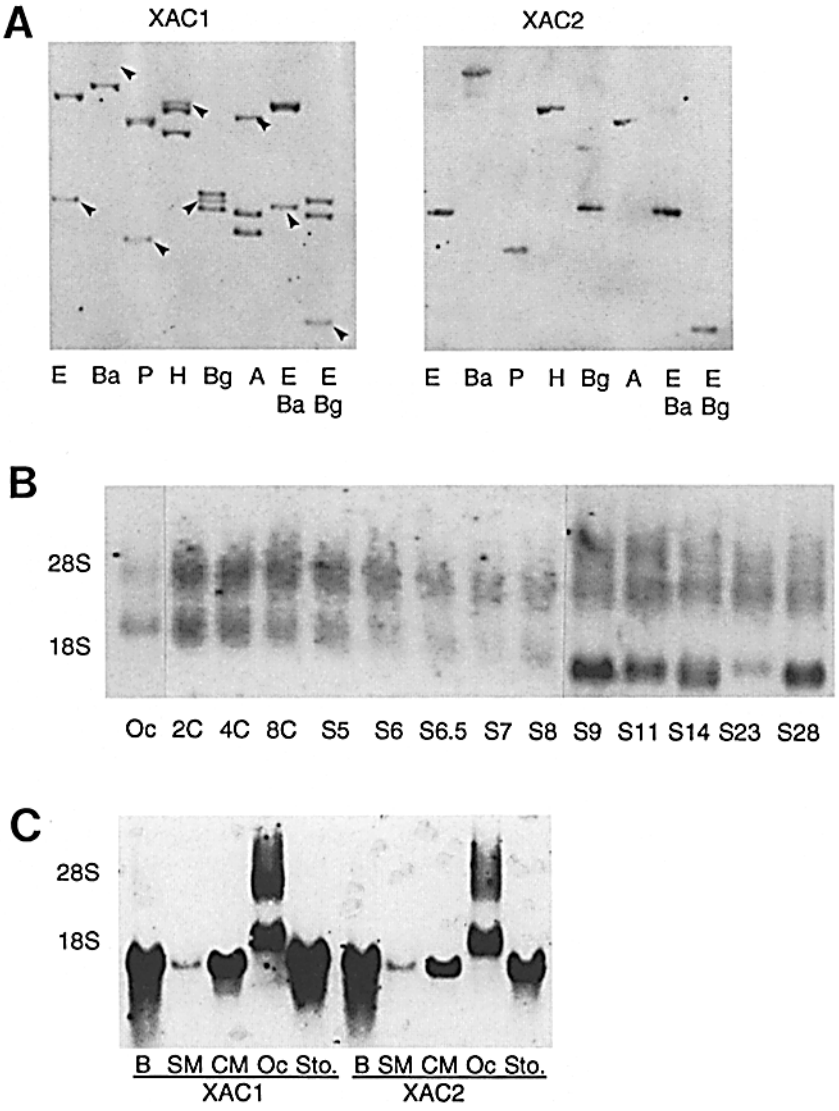

Figure 3. (*A*) Southern blots of *Xenopus* genomic DNA hybridized to XAC1 and XAC2 3′UTR DNA probes (see Fig. 1). Restriction endonucleases used: *E*, EcoRI; *Ba*, BamHI; *P*, PstI; *H*, HindIII; *Bg*, BglII; *A*, ApaI. Arrowheads show the XAC2 genomic DNA bands which are cross-reactive with XAC1 probe. (*B*) Northern blot of total RNA (13 μg/lane) from unfertilized eggs (*Oc*) and developing embryos hybridized to coding region DNA probe for XAC1. Two, four, and eight cell embryos (*2C*, *4C*, and *8C*); other developmental stages are shown by the stage number. Positions of 18 S and 28 S ribosomal RNA remained constant across the gel (visualized by ethidium bromide staining) while those of the XAC mRNAs decreased to the adult sizes. Identical results were obtained using the 3′UTR DNA probes (not shown). Lanes *S9–S28* were from a separate gel (longer exposure) that also contained oocyte RNA and were aligned accordingly. Because of the overlap in the signal with the rRNA bands before stage 9, it is not possible to conclude from this gel alone that the signals are specific. However, immunoblotting and immunofluorescence staining reported below support the early expression seen here. (*C*) Northern blot of total RNA (13 μg) from adult tissues hybridized to 3′UTR DNA probes of XAC1 (*left*) and XAC2 (*right*). Ethidium bromide staining (not shown) was used to verify that similar amounts of RNA were loaded per lane. These results demonstrate both the specificity of probe hybridization to the 4.5-kb mRNA, and the difference in size of the smaller mRNA between oocyte and adult. Identical results were obtained using the coding region DNA probe for XAC1 used in Fig. 3 *B* (not shown). *B*, brain; *SM*, skeletal muscle; *CM*, cardiac muscle; *Oc*, oocytes removed from adult; *Sto*, stomach.

pernatant at both pHs. The uncleaved chimeric proteins had similar F-actin depolymerizing activity to recombinant chick ADF or cofilin when assayed at pH 8.0 and expressed as G-actin released per ADF/cofilin equivalent (Fig. 2 *C*).

Two Embryonic cDNAs Probably Represent Allele Variants

The high homology within the coding region of the two XAC cDNAs precluded using the whole cDNAs as probes to distinguish between the 2 XAC genes and 2 mRNAs. The greatest differences between the two XAC cDNAs occur in the 3′UTR, so probes were prepared encompassing bases 906-1482 for XAC1 and 1055-1507 for XAC2. Southern blots (both single and double digests) of *Xenopus* genomic DNA (Fig. 3 *A*) show the XAC2 probe could be made specific for the XAC2 gene. However, the XAC1 probe always cross-hybridized to the XAC2 gene (Fig. 3 *A*). Nevertheless, it is clear that each XAC cDNA arises from a separate gene.

Northern blots of total RNA extracted from different stages of developing embryo (Fig. 3 *B*) and from adult tissues (Fig. 3 *C*) showed identical patterns when hybridized to either the specific XAC2 probe or the cross-reactive XAC1 probe, suggesting that both XAC mRNAs are coordinately expressed. Levels of XAC mRNA of 1.8 kb were high in brain, heart, oocyte, stomach and low in skeletal muscle. mRNAs of 2.5 kb and 4.5 kb were identified in oocytes by hybridization to either XAC probe. These migrated nearly identically to 18 and 28 S rRNA until stage 9. The 4.5-kb species was not found in adult tissues. The maternal 2.5-kb species was gradually replaced by a 1.8-kb size (the adult tissue size) between the morula and tadpole (stages 5 to 34).

The same 3′-UTR region of each XAC cDNA used for probing Southern and Northern blots was used to generate digoxigenin-labeled antisense riboprobes to examine the distribution of the mRNAs during *Xenopus* development by in situ hybridization (Fig. 4). Sense riboprobes were used as controls. Both XAC mRNAs are concentrated at the anterior end and along the dorsal side of the developing embryo. Nerve tissue, including the brachial arches, neural plate, neural tube, and retina, show particularly high expression. The protruding cement gland, visible after stage 26, does not contain XAC mRNA, but the cell bodies which generate this neurite rich region stain brightly for XAC protein (see below).

To distinguish between the XAC1 and XAC2 proteins, specific antibodies (Table I) were raised to KLH-conjugated synthetic decapeptides from the region of the two species (residues 124-133) with the greatest sequence differences (Fig. 1 *B*). Antiserum to the peptide from XAC1 cross-reacted with GST-XAC2, but could be made specific for XAC1 by using antibodies isolated on an XAC1-peptide affinity column and by washing immunoblots in 0.4 M $MgCl_2$ for 5 min after the primary incubation step, to dissociate weak complexes (Fig. 5 *A*). Antiserum to XAC2 did not cross-react with GST-XAC1, but it did cross-react with several other proteins in *Xenopus* tissue extracts. This nonspecific cross-reactivity could be reduced, but not eliminated, by immunoabsorbing the antiserum with KLH

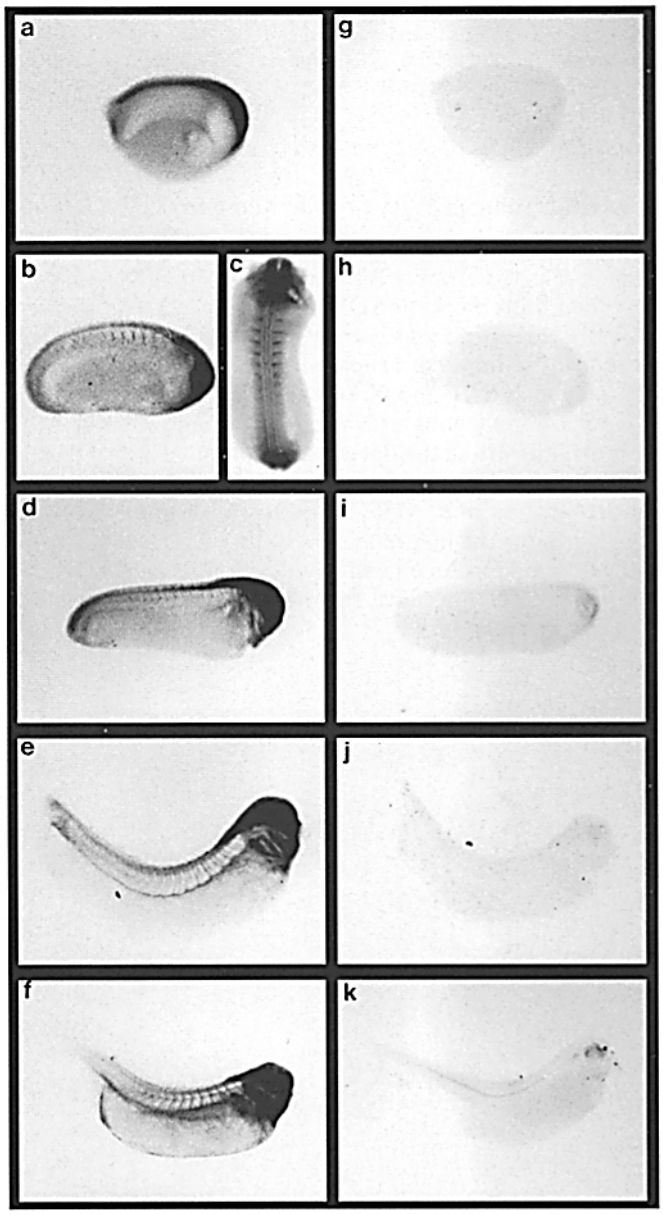

Figure 4. In situ hybridization of *Xenopus* embryos with XAC riboprobes. Identical patterns of expression were observed with the specific probe to the 3′UTR of XAC2 and with the coding region probe to XAC2 (cross-reacts with XAC1 gene fragments on Southern blots). The anti-sense RNA probe used for *a*, *b*, *d*, *e*, and *f* is from the XAC2 coding region, while the XAC1 3′UTR probe was used for *c* (the dorsal view). Controls (*g–k*) use the sense RNA probes made against the coding region of XAC2. Developmental stages shown: 15/16 (*a* and *g*); 21 (*b*, *c*, and *h*); 26 (*d* and *i*); 32 (*e* and *j*); 36 (*f* and *k*). The development of the reaction product was stopped quickly to show the regions that contained particularly high levels of the XAC mRNA. It is difficult to differentiate specific regions within the head from these studies, but immunofluorescence localization of the XAC was done on vertical sections through the anterior end of the embryo (see below).

(1 mg/ 200 μl serum) and purifying the antibodies on an XAC2-peptide affinity column (Fig. 5 *A*). Because of residual nonspecific cross-reactivity with other proteins, immunostaining of a band of the correct molecular size for XAC cannot be unambiguously interpreted as indicating

Table I. Characterization of the Different XAC Antibodies Used Here

Antigen	Animal	Name	Polyclonal (PC) or monoclonal (M)	Specificity	Used in figure no.
CGGIKKRLPGIKH (peptide from XAC1)	rabbit	XAC1 peptide Ab	PC	XAC1	5, *A*, *B*, and *C*
CGGIRKRFTGIKH (peptide from XAC2)	rabbit	XAC2 peptide Ab	PC	XAC2 and other proteins, but not XAC1	5, *A*, *B*, and *C*
GST-XAC1	rabbit	PC-IgG	PC	XAC1 and XAC2	5 *D*, 9 *a*
GST-XAC1	rat	1A11	M	XAC1 and XAC2 (weak reactivity with a few other Xenopus proteins)	8, 11
GST-XAC2	rat	2F10	M	XAC1 and XAC2	6, 7, 10 *d*

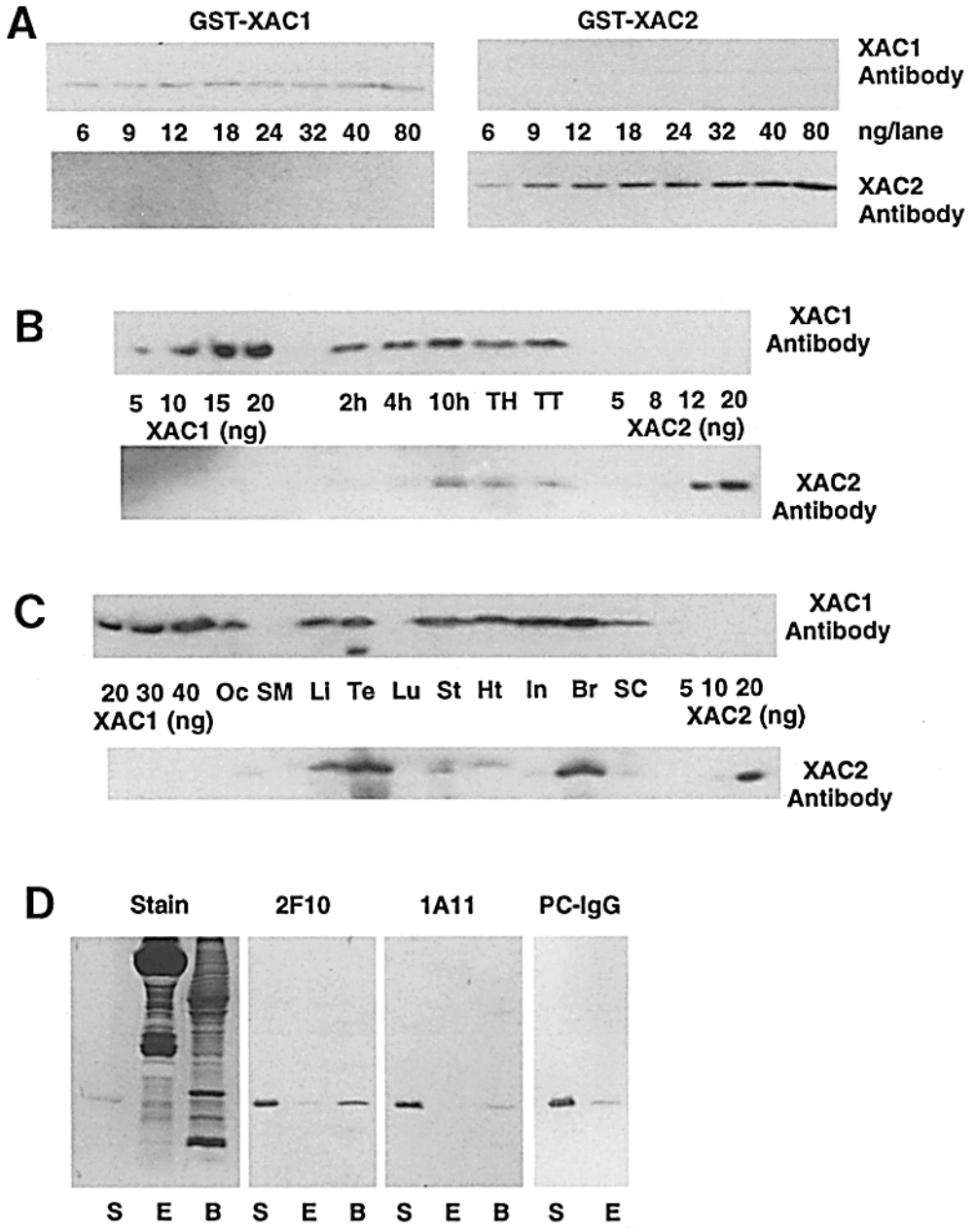

Figure 5. (*A*) Specificity of rabbit antiserum raised to peptides from XAC1 and XAC2 tested against different amounts of GST-XAC1 and GST-XAC2 on Western blots. Both antisera were used at 1:1,000 dilutions and the blots using XAC1 peptide antibody were washed in 0.4 M $MgCl_2$ to improve specificity. (*B*) Western blot of extracts (2 μg protein) from embryos made at 2, 4, and 10 h postfertilization, and from tadpoles 72 h after fertilization probed with XAC1 and XAC2 peptide antibodies. *TH*, tadpole head; *TT*, tadpole tail. To show antibody specificity, standards of thrombin-cleaved GST-XAC1 and GST-XAC2 are loaded on the left and right hand sides of the gel, respectively, with the amounts shown as ng/lane of XAC. (*C*) Western blots, probed with XAC1 and XAC2 peptide antibodies, of extracts from: *Oc*, unfertilized eggs; *SM*, skeletal muscle; *Li*, liver; *Te*, testis; *Lu*, lung; *St*, stomach; *Ht*, heart; *In*, intestine; *Br*, brain; *SC*, spinal cord. All extracts contained 10 μg protein except for brain and spinal cord which contained 5 μg protein. Position of standards is as in *B* with the amounts shown as ng/lane of XAC. (*D*) Specificity of monoclonal antibodies (hybridoma supernatants) 2F10 and 1A11, and polyclonal (*PC*) IgG raised against GST-XAC, tested against XAC1 standard (*S*) and extracts of *Xenopus* stage 21 embryos (*E*) and adult brain (*B*). Coomassie blue–stained gel (Stain) and Western blots are shown. XAC1 standard was prepared by thrombin cleavage of GST-XAC1.

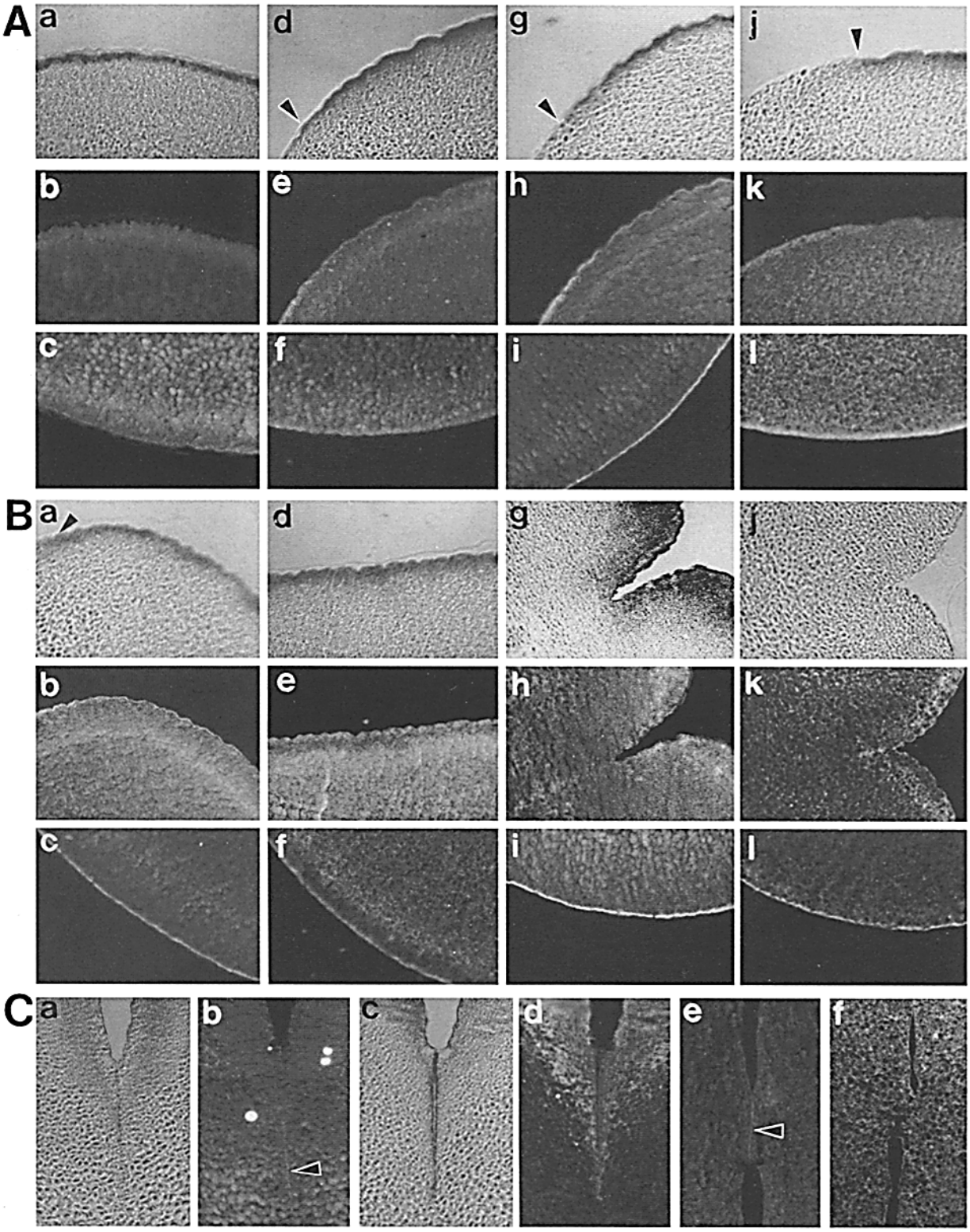

Figure 6. Immunofluorescence localization of XAC (using monoclonal antibody 2F10) and actin in 5 μm sections of *Xenopus* oocytes, eggs, and embryos. Photographic and printing times were adjusted such that sections stained with secondary antibody alone (control for monoclonal antibody) or nonimmune rabbit serum (control for actin polyclonal antibody) were black. (*A*) Oocytes (*a–c*), unfertilized eggs (*d–f*), and zygotes 30 min after fertilization (*g–l*). Phase contrast micrographs showing the junction (*arrowheads*) between the animal and vegetal hemisphere cortex (*a*, *d*, *g*, and *j*) and corresponding immunofluorescence (*b*, *e*, *h*, and *k*) showing both XAC (*b*, *e*, and *h*) and actin (*k*). Immunofluorescence of the cortex within the vegetal hemisphere showing XAC (*c*, *f*, and *i*) and actin (*l*). (*B*) Sections of zygotes at 1 h postfertilization (*a–f*) and during early first cleavage (*g–l*). Phase contrast micrographs showing the animal hemisphere (*a*, *d*, *g*, and *j*) (arrowhead in *a* shows junction between hemispheres) and corresponding immunofluorescence for XAC (*b* and *h*) and

the presence of XAC2. However, the lack of staining is a good indication that XAC2 is not present. Western blots of extracts from different stages of developing embryos (Fig. 5 *B*) and mature frog tissues (Fig. 5 *C*) strongly suggest that the two isoforms are coordinately expressed. Neither XAC1 nor XAC2 was detected in extracts of skeletal muscle or lung, suggesting they have the same tissue specific distribution. Taken together, these results strongly suggest that XAC1 and XAC2 are allelic variants.

Immunocytochemical Localization of XAC during Development

The cross-reactivity of the peptide-specific polyclonal antibodies with other *Xenopus* proteins precluded their use in immunocytochemistry. Therefore, monoclonal antibodies were prepared by immunizing a rat with the recombinant GST-XAC2 chimera and fusing the rat lymph node cells with mouse myeloma cells. Two clones were eventually established which recognized epitopes in common between XAC1 and XAC2. One clone, 2F10, required conditioned medium and IL-6 supplementation for growth but it produced antibodies highly specific for XAC in tissue extracts (Fig. 5 *D*). The second clone, 1A11, grew well without special supplements and produced antibodies which also recognized XAC1 and 2, but these antibodies also cross-reacted weakly with other proteins in *Xenopus* brain extracts (Fig. 5 *D*). This latter hybridoma line produced antibodies useful for immunoblot analysis but not for immunocytochemistry. In addition, a rabbit antiserum was also raised against the GST-XAC1 and the IgG fraction was purified on protein A–agarose. This IgG was specific for XAC (both forms) in tissue extracts (Fig. 5 *D*). This IgG was used below for embryo injection studies.

X. laevis eggs and embryos, fixed at various stages of development, were immunostained for XAC using the specific monoclonal antibody, 2F10. Immunofluorescent localizations of XAC and actin in 5 μm sections of oocytes, unfertilized eggs, and zygotes are shown in Fig. 6 *A*. XAC staining is diffuse in the cortical cytoplasm of oocytes in both the animal and vegetal hemispheres (Fig. 6, *A-b* and *c*). In the unfertilized eggs there is increased immunofluorescence associated with the membrane, particularly in the vegetal hemisphere (Fig. 6, *A-e* and *f*), although most staining is still diffuse. Sections from different unfertilized eggs showed the largest variability in XAC distribution, perhaps related to the variability observed in XAC phosphorylation state (see below). 30 min after fertilization (Fig. 6, *A-h* and *i*) there is enhanced immunostaining of the membrane, especially in the vegetal hemisphere, at regions where actin immunofluorescence is also strong (Fig. 6, *A-k* and *l*). Immunofluorescence also is brighter at the junction between the cortical cytoplasm and the animal hemisphere cytoplasm (Fig. 6 *A-h*). 1 h after fertilization (before first cleavage) the staining for XAC at the junction between cortical cytoplasm and animal hemisphere cytoplasm is even more pronounced (Fig. 6 *B-b*). Actin staining is reduced in the cortical cytoplasm (Fig. 6, *B-e* and *f*) and brighter in the animal hemisphere cytoplasm (Fig. 6 *B-e*) at this stage. Early in the first cleavage, XAC staining accumulates around the cleavage furrow (Fig. 6 *B-h*) and along the vegetal membrane (Fig. 6 *B-i*). Actin immunofluorescence is bright in both these regions as well (Fig. 6, *B-k* and *l*). Late in first cleavage, XAC immunofluorescence is found in the midbody structure (Fig. 6, *C-a* and *b*), staining deeper in the furrow than the bulk of the actin (Fig. 6, *C-c* and *d*). Staining of this midbody structure for XAC but not actin persists through the end of first cleavage (Fig. 6, *C-e* and *f*). Identical results for XAC distribution were obtained using the XAC polyclonal antibody (not shown).

Whole mount immunochemical staining of albino *Xenopus* embryos for XAC shows staining at the boundary of the blastomeres where cleavage from the two cell to the four cell stage is going to occur (Fig. 7 *a*) or around the boundary of the cells after the 8 cell stage (Fig. 7 *b*). In these specimens, development of the alkaline phosphatase reaction product was stopped at an early stage to allow the visualization of regions of highest concentration. Controls (second antibody alone) showed no staining (not shown). At the blastula stage, cells on the animal sphere were strongly stained and most cells, except those of the yolk plug, were highly positive during gastrulation (not shown). Staining was found in most tissues of the stage 38 embryo with the heaviest staining in the nervous system and retina (Fig. 7 *c*). Controls (secondary antibody alone—not shown) looked virtually identical to those from the in situ hybridization experiment (Fig. 4 *k*).

Additional immunofluorescence staining for XAC with the monoclonal antibody 2F10 was done on sections from embryos at stage 17, 24, and 34. By stage 17 (Fig. 7 *d*), the XAC is concentrated in cells of the developing neuroectoderm. Cells within the notochord, neural tube, neural crest, somites, and around the lumen of the archenteron, as well as a layer of cells in the archenteron, stain very brightly for XAC at stage 24 (Fig. 7, *e* and *f*). By stage 34, staining intensity had declined in the notochord, but the neural tube, epidermis and a layer of cells in the archenteron stain brightly (Fig. 7 *g*). A more anterior vertical section of the same stage embryo (Fig. 7 *h*) shows very bright staining throughout the developing retina, and in the cell bodies of the neurons at the base of the cement gland which are also derived from neuroectoderm. Immunofluorescence in the micrographs shown has been adjusted to correct for background staining with secondary antibody alone (black image).

Phosphorylation of XAC Changes Dramatically during Early Development

Two dimensional immunoblots of extracts from *Xenopus* embryos and adult tissues show the presence of two immu-

actin (*e* and *k*). Immunofluorescence of vegetal hemisphere cortex stained for XAC (*c* and *i*) and actin (*f* and *l*) are also shown. (*C*) Phase contrast micrographs (*a* and *c*) and corresponding immunofluorescence for XAC (*b*) and actin (*d*) in sections of the zygotes at late first cleavage. Arrowhead in *b* shows staining of the XAC preceding the invagination of the cleavage furrow. Immunofluorescence of XAC and actin in sections of the blastocysts at the end of first cleavage are shown in *e* and *f*, respectively. Staining of a midbody structure for XAC is shown by arrowhead.

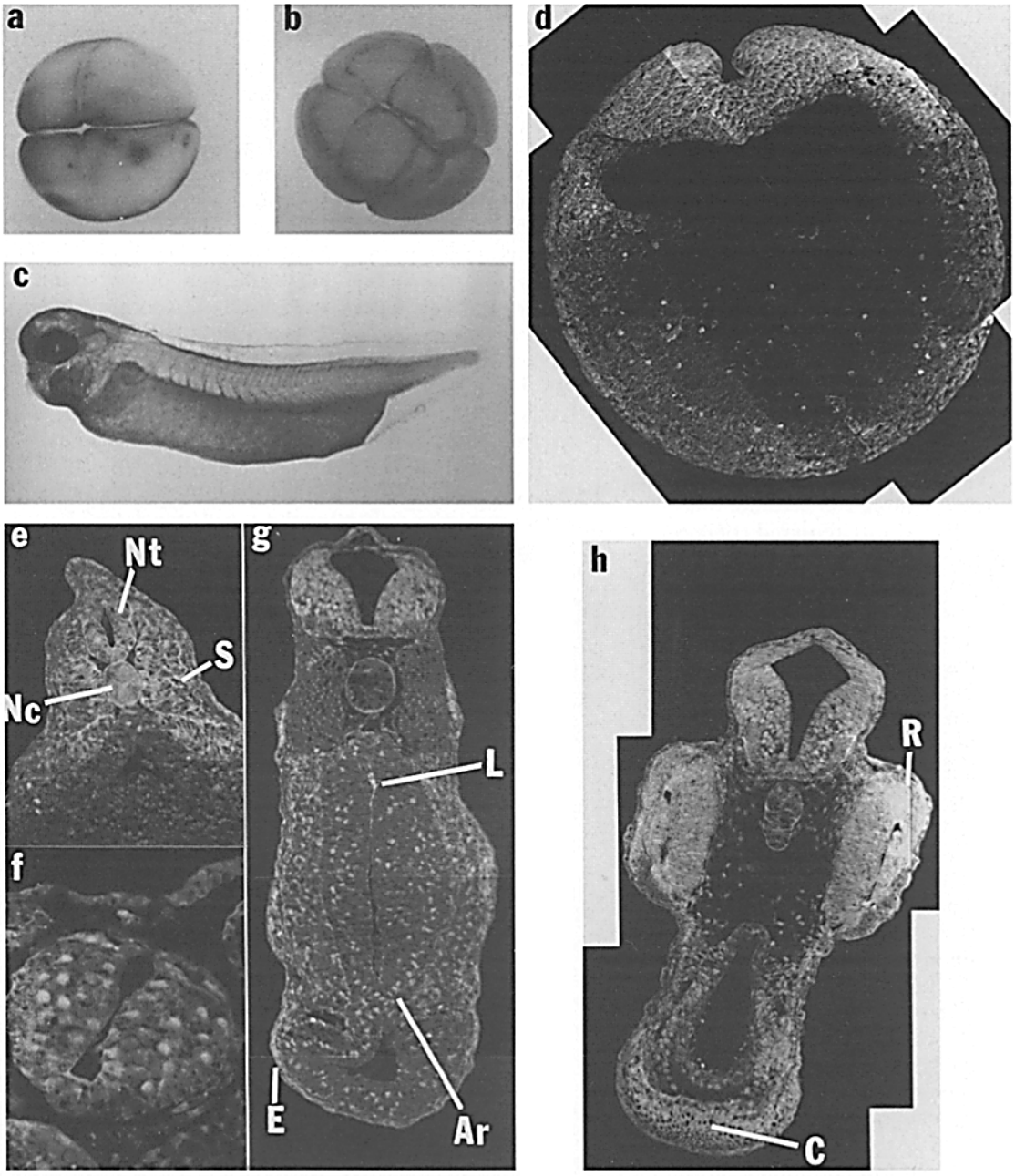

Figure 7. Immunocytochemical staining for XAC (using the 2F10 monoclonal antibody) in whole mount (albino) *Xenopus* embryos during development. Stages shown are (*a*) 2 cell, (*b*) 8 cell, and (*c*) stage 38. Development times were limited to allow visualization of the regions of most intense staining. No staining was observed in embryos treated with secondary antibody alone. Immunofluorescence staining of XAC in 5 μm vertical sections of developing (wild type) *Xenopus* embryos. Stage 17 embryo (*d*) shows particularly strong fluorescence for XAC in the region of the developing neural plate and neural fold. Cells within the neural tube (*Nt*), notochord (*Nc*) and somites (*S*) are brightly stained at stage 24 (*e*). (*f*) An enlargement of the neural tube from a stage 24 embryo shows many brightly stained cells. (*g*) The neural tube, epidermis (*E*), cells lining the lumen of the archenteron (*L*), and a layer of cells within the archenteron (*Ar*) are brightly stained at stage 34. A more anterior vertical section through a stage 34 embryo (*h*) shows intense staining of the neural tube, cells within the developing retina (*R*) and the neuronal cell bodies which constitute the base of the cement gland (*C*). Immunofluorescent controls (secondary antibody only) for sections of oocyte and embryos were black (not shown).

noreactive species, with mobilities similar to phosphorylated and dephosphorylated forms of chicken ADF (Morgan et al., 1993). The more acidic species in the *Xenopus* embryonic extract (pXAC) is converted to the dephosphorylated form by treatment with alkaline phosphatase (Fig. 8 *A*). Two dimensional immunoblots of extracts from embryos at different stages of development from a single batch of fertilized eggs show a rapid dephosphorylation of pXAC occurs after fertilization (Fig. 8 *B*). A systematic analysis of these changes during development (Fig. 8 *C*) shows that oocytes, surgically removed from the adult, contained only pXAC. In unfertilized eggs, pXAC com-

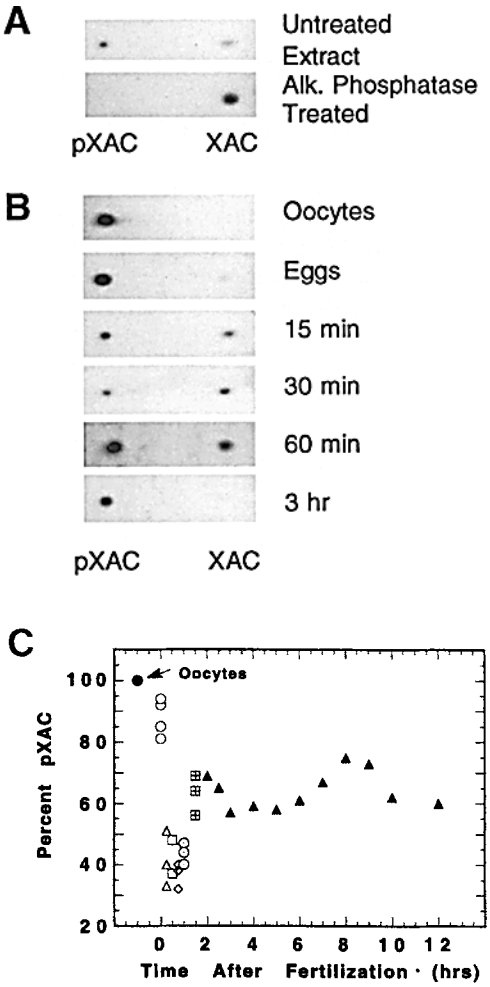

Figure 8. (*A*) Immunoblot of 2D gel (NEpHGE/SDS-PAGE) of extracts from *Xenopus* zygote (1 h post fertilization) before and after treatment of the denatured proteins with alkaline phosphatase (Morgan et al., 1993). (*B*) Immunoblots of 2D gels of oocytes, unfertilized egg, and fertilized eggs at 15, 30, 60 min, and 3 h postfertilization. (*C*) pXAC as a percent of total immunoreactive XAC quantified from 2D immunoblots of embryo extracts. Each solid triangle represents values from at least three 2D gels of pooled embryos (5–10) taken at the times shown after mass fertilization of eggs. Open symbols represent values from individual eggs or embryos at 0-, 15-, 30-, 60-, and 180-min time points to show individual variability. In individual oocytes removed surgically from the adult (●), pXAC was the only immunoreactive species present ($n = 8$).

prises 80–95% of the total XAC, and this drops rapidly within 30 min after fertilization to give a greater abundance of the dephosphorylated form. During the first few hours of development, when division is synchronous, variability was seen between embryos, especially between those collected on different days. Since the rate of early development is very temperature dependent, the variability in the phosphorylation state of XAC may reflect changes which occur during the cell cycle. Such changes are suggested by studies on a single batch of fertilized eggs (Fig. 8 *B*) which show the initial dephosphorylation of pXAC is followed by rephosphorylation at 3 h. When division synchrony is lost, variability in pXAC content between individual embryos decreases. In pooled embryos, pXAC increases again in abundance between the morula and blastula stages (5–8 h postfertilization), and then decreases again as gastrulation is approached (~12 h).

Microinjection of Anti-XAC IgG and GST-XAC Inhibits Cytokinesis

Injection of anti-XAC IgG into one blastomere of embryos at the 2 cell stage inhibited cleavage of the injected blastomere (Fig. 9 *a*). This abnormal phenotype was observed in 94% (78/83) of embryos injected with 20 nl of 15

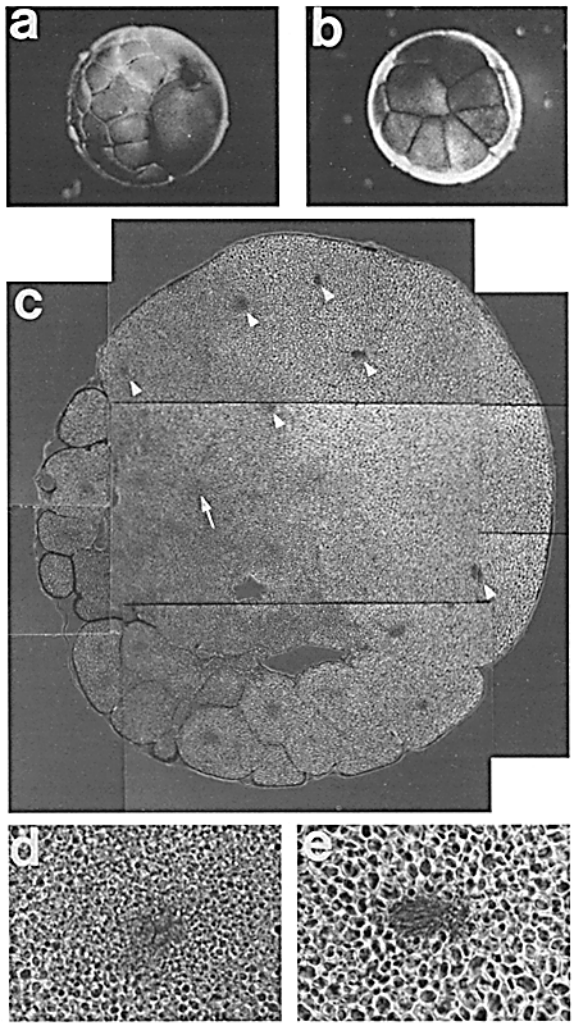

Figure 9. Inhibition of XAC with antibody or introduction of constitutively active GST-XAC inhibits cleavage of Xenopus embryos. (*a*) Anti-XAC (PC-IgG) (10 mg/ml; 20 nl) was injected into one blastomere of *Xenopus* embryos at the two cell stage. Cleavage of the injected blastomere was inhibited as shown. Embryos were allowed to develop for 3 h before photography. Injected hemisphere is on the right side of embryo. (*b*) Embryo injected with anti-XAC (PC-IgG) which had been neutralized with GST-XAC before injection. Development is normal (16 cell stage). (*c*) Phase contrast micrographs of 6 μm cross-section of animal hemisphere of embryo injected in one blastomere at the two cell stage with anti-XAC (PC-IgG) (10 mg/ml; 20 nl). Embryos were fixed 3.5 h postinjection. Lobed cleavage nucleus is shown by an arrow and is magnified in *d*. Asters are shown by arrowheads and magnified in *e*.

mg/ml IgG, 84% (52/62) embryos injected with 20 nl of 10 mg/ml IgG, and 55% (36/66) embryos injected with 20 nl of 7 mg/ml IgG. Normal development (to gastrula stage) occurred in 84% (58/69) of blastomeres injected with anti-XAC IgG (20 nl of 10 mg/ml), neutralized before injection with an excess of GST-XAC (Fig. 9 *b*), and in 75% of embryos injected with nonimmune IgG at 10 mg/ml. Nuclear division was not inhibited in the cleavage deficient blastomere (Fig. 9 *c*). Both lobed cleavage nuclei (Fig. 9 *d*) and asters (Fig. 9 *e*) were observed suggesting that XAC is not required for karyokinesis.

Cleavage was also blocked in 68% (23/34) of blastomeres injected with GST-XAC (5 mg/ml; 20 nl) (Fig. 10 *a*). Since cytokinesis seemed to be blocked by either too much or too little XAC activity, we injected eggs undergoing the first cleavage with the GST-XAC to see what effect this had on furrow formation. Eggs injected with buffer alone completed cleavage normally whereas those injected with GST-XAC underwent regression of the cleavage furrow (Fig. 10 *b*). Paraffin sections of eggs in which the cleavage furrow disappeared after GST-XAC injection sometimes showed regions of reduced pigment density at the membrane where the furrow had originally formed (Fig. 10, *c* and *e*) and pigment granules were deposited deeper within the cytoplasm. Actin staining was diffuse in the cortex above the deposited pigment granules (Fig. 10 *d*). Other injected eggs showed pigment both at the surface and deposited in the regressed furrow (Fig. 10 *e*) with strong immunofluorescence staining of the XAC in the cortex (Fig. 10 *f*). These results suggest that XAC is needed to form the cleavage furrow, but that excess active XAC destroys the contractile ring.

Injection of chick brain ADF (3 mg/ml) into eggs did not inhibit development (not shown) suggesting that the GST-XAC, unlike brain ADF, is unable to be inactivated by phosphorylation. This was examined directly by injecting eggs with brain ADF or GST-XAC1, and, after 1 h, extracting the proteins for analysis by 2D immunoblotting. One part of the sample was treated with alkaline phosphatase before running the 2D gels. Brain ADF was phosphorylated and the pADF disappeared after phosphatase treatment (not shown). The position of recombinant GST-XAC1, visualized with the 1A11 antibody (Fig. 11 *a*), was not altered by injection into fertilized eggs (Fig. 11 *b*). Furthermore, no change in the pattern of staining of the GST-XAC was observed after alkaline phosphatase treatment under conditions which completely dephosphorylated all of the endogenous pXAC (Fig. 11 *c*). Thus, the GST-XAC is not susceptible to phosphorylation in vivo and, therefore, serves as a constitutively active form of XAC.

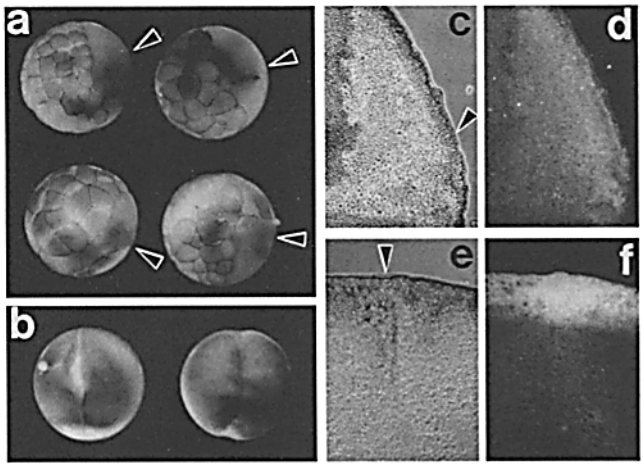

Figure 10. (*a*) GST-XAC (5 mg/ml; 20 nl) was injected into one blastomere of 34 embryos at the 2 cell stage. Cleavage of the injected blastomere was inhibited in 68% of the embryos. Four representative examples are shown with arrowheads pointing to the injected blastomere. (*b*) Injection of GST-XAC (5 mg/ml; 20 nl) into an egg undergoing first cleavage causes the regression of the cleavage furrow (*left*, fixed in the process of regression) whereas injection of buffer had no effect (*right*). (*c–f*) Phase contrast and immunofluorescence photographs of paraffin sections of eggs microinjected with GST-XAC during first cleavage and fixed after furrow regression. (*c* and *e*) Phase contrast photographs show position of regressed cleavage furrow (*arrowheads*). Pigment granules were often depleted in region of regressed furrow with pigment granules remaining deeper in cytoplasm. (*d*) Immunofluorescence staining of actin in the same section of regressed furrow shown in *c*. Actin fluorescence is diffuse in the cortex. (*f*) Immunofluorescence staining of XAC (using 2F10 monoclonal antibody) of the same section of regressed furrow shown in *e*. The XAC is also diffuse in the cortex of the injected egg.

Discussion

Results clearly demonstrate that the two *Xenopus* cDNAs we have cloned and expressed represent members of the ADF/cofilin family of proteins. Although these proteins have a greater similarity in sequence to other vertebrate cofilins than to vertebrate ADFs, we have elected to refer to them by the family name, *Xenopus* ADF/cofilin (XAC). This name is more descriptive of the two activities shared by all of the vertebrate proteins in this family, i.e., the ability to depolymerize F-actin and the ability to bind to, and cosediment with, F-actin in a pH-dependent manner (Bamburg et al., 1980; Nishida et al., 1984; Yonezawa et al., 1985; Hayden et al., 1993; Hawkins et al., 1993).

Although XAC1 and XAC2 arise from different genes, they have a high degree of sequence homology both within and outside of the coding region. Results from Northern blots, in situ hybridization, and Western blots indicate that both XAC1 and XAC2 are expressed in the same tissues and at the same time during development. Taken together, these results strongly suggest that XAC1 and XAC2 are allelic variants, probably arising from the pseudotetraploid state of *X. laevis*, estimated to have arisen about 30 million years ago (Bisbee et al., 1977).

The adult tissue distributions of these XACs are similar, but not identical, to that found for chicken ADF (Bamburg and Bray, 1987). For instance, high amounts of these proteins are found in nerve tissue (brain and spinal cord), intestine, and liver from adult frog and chicken, and the proteins are not detectable in extracts of adult skeletal muscle from either animal. On the other hand, lung tissue from adult chicken contained ADF, but XAC was not detectable in *Xenopus* lung, and adult chicken cardiac muscle did not contain significant amounts of ADF, whereas protein and RNA extracts of *Xenopus* cardiac muscle gave strong XAC bands on Western and Northern blots, respectively. The significance of these differences is not

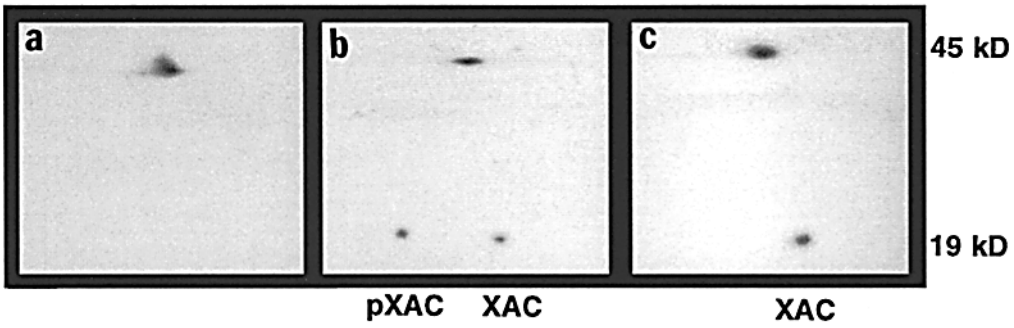

Figure 11. GST-XAC is not phosphorylated in *Xenopus* eggs. Fertilized eggs were microinjected with GST-XAC1 (4 mg/ml; 30 nl/egg) and 1 h later the eggs were extracted, proteins precipitated, and half of the sample treated with alkaline phosphatase as described in Materials and Methods. Samples and a standard of uninjected protein were separated by 2D gel electrophoresis and immunoblotted using the 1A11 monoclonal antibody to XAC. (*a*) Recombinant GST-XAC1 before injection. (*b*) Extracts from eggs injected with GST-XAC1 show the two endogenous XAC species (pXAC and XAC) and a single spot of 45 kD for GST-XAC1. (*c*) Alkaline phosphatase treatment of this extract completely converted the endogenous pXAC to XAC, but the position of the GST-XAC1 did not change.

known at this time, but it is possible that other isoforms of these proteins (Ono et al., 1994) are present in different adult tissues.

XACs are encoded by maternal mRNAs, which suggests that these proteins have important roles in early embryonic development. The diffuse cytoplasmic distribution of the XAC in the oocyte is consistent with its presence in an inactive (phosphorylated) form. In the unfertilized egg, in which ~20% of the XAC is in the unphosphorylated state, there is a clear localization of some of the XAC to the membrane, especially that of the vegetal hemisphere. After fertilization, a rapid decline in the level of pXAC occurs which correlates with an increased localization of the XAC to the membrane, particularly in the vegetal hemisphere, and to the junction between the cortical cytoplasm and the cytoplasm of the animal hemisphere. This relocalization precedes cortical rotation, which defines the dorsal/ventral axis of the developing embryo (Vincent et al., 1986; Vincent and Gerhart, 1987). Pharmacological studies on *Xenopus* oocytes have suggested that cortical rotation is restricted by actin filaments and is dependent upon microtubules (Manes et al., 1978), although the exact mechanism of the phenomenon has not yet been elucidated. If actin filaments are involved in restricting the cortical rotation, the localization of the XAC to the interface between the cortical and animal hemisphere cytoplasm suggests that it may play a role in the breakdown of the actin filaments, and that its correct temporal activation after fertilization is what regulates the timing of the rotation. Such a role would be important in establishing the dorsal/ventral axis in amphibian embryos. Direct experiments to test this hypothesis are in progress.

The localization of the XAC in the cleavage furrow and midbody structure of dividing *Xenopus* cells is not surprising in view of the recent localization of cofilin in the cleavage furrow of mammalian cells undergoing cytokinesis (Nagaoka et al., 1995). The finding that XAC is found deeper within the furrow than the bulk of the actin suggests that XAC associates with a subset of F-actin (for review see Fishkind and Wang, 1995), possibly filaments which do not contain tropomyosin, a known inhibitor of ADF (Bernstein and Bamburg, 1982; Bamburg and Bernstein, 1991) and cofilin (Nishida et al., 1984). It has been proposed (Nagaoka et al., 1995) that the late arrival of the mammalian cofilin into the cleavage furrow accompanies the disassembly of actin filaments in the contractile ring, which occurs as cytokinesis progresses (Singal and Sanders, 1974). Such a role would be consistent with the effects of constitutively active XAC (e.g., GST-XAC), which in excess is able to destroy the contractile ring and cause cleavage furrow regression. Embryos injected with chick brain ADF (Verrastro, T.A., M.D. Brown, and J. R. Bamburg, unpublished results) appear to be able to handle the higher levels by inactivating the protein by phosphorylation. However, GST-XAC is not phosphorylated in vivo, which suggests that cell cycle regulation of XAC activity by phosphorylation may control the reorganization of actin involved in cytokinesis. Alterations in XAC phosphorylation during the cell cycle may also explain the variability seen in the amount of pXAC in individual embryos, since progression through the cell cycle was timed from sperm addition and fertilization is not instantaneous. The variation in pXAC levels observed between individual eggs could also arise from differential mechanical effects of the dejellying procedure.

It was surprising to find that the GST-chimeric constructs with XAC have full F-actin depolymerizing activity. GST, a protein of ~26 kD, is on the NH_2 terminus of the XAC. The position of the regulatory phosphorylation site in mammalian ADF/ cofilins is Ser 3 in the encoded proteins (Agnew et al., 1995; Moriyama et al., 1996). One might expect that such a large NH_2-terminal extension would perturb the structure at least as dramatically as the addition of a phosphate group to Ser 3. The fact that these proteins have full activity in vitro suggests that chimeric constructs of the XAC with the 25-kD green fluorescent protein (GFP) (Chalfie et al., 1992), could prove useful in examining the localization of active XAC in vivo. However, since we show that XAC with such an NH_2-terminal extension is not recognized by the endogenous kinase, it will not be regulated normally in vivo.

The modulation of activity of vertebrate ADF/cofilins by phosphorylation has been established as a major in vivo regulatory mechanism (Morgan et al., 1993; Agnew et al., 1995). The phosphorylated isoform is inactive in binding to monomeric actin or depolymerizing F-actin (Morgan et al., 1993). In astrocytes (Baorto et al., 1992), thyroid cells (Saito et al., 1994), platelets (Davidson and Haslam, 1994), T-lymphocytes (Samstag et al., 1994), and neutrophils (Suzuki et al., 1995), dephosphorylation of ADF/cofilin ac-

companies dramatic changes in the actin cytoskeleton important for cellular function (for review see Moon and Drubin, 1995). Here we show that phosphorylation control of XAC activity occurs during early embryonic development as well. Since the inactivation of XAC in eggs with antibody prevents cytokinesis, the activation of XAC by dephosphorylation which follows fertilization is a critical step in early *Xenopus* development.

Although the XACs appear to be widely distributed within the embryo after gastrulation, their very high concentration within the neuroectoderm and continued presence in neural tissues suggest they play an important role in neurogenesis. In vertebrate neurons, proteins in the ADF/cofilin family are found enriched in growth cones of both axons and dendrites both in vivo (Léna et al., 1991) and in vitro (Bamburg and Bray, 1987). These proteins appear earlier in development and with a broader neuronal distribution than has been found for the actin monomer-binding peptide, thymosin β4 (Yamamoto et al., 1994), although there may be other low molecular weight actin-binding proteins in *Xenopus* cytoplasm (Rosenblatt et al., 1995). The early expression and broad neuronal distribution make the ADF/cofilin proteins likely regulators of the dynamic actin filaments involved in growth cone motility, pathfinding, and synaptogenesis. The *Xenopus* system offers an excellent experimental model in which to further examine their regulation and role in early development and neurogenesis.

The authors gratefully acknowledge the suggestions and support of Mauricio X. Zuber who helped us initiate this project before his tragic death in June, 1994. We would like to thank his former student, Dr. Dan Shain, for use of his *Xenopus* library. We thank Dr. Ichiro Yahara, Tokyo Metropolitan Institute of Medical Science for the polyclonal anti-actin antibody. The authors gratefully acknowledge the technical contributions of Todd Verrastro, Michael Brown, Brian Agnew, Judith Sneider, and Hui Chen to various aspects of this work.

This work was supported in part by National Institutes of Health grant GM35126 to J.R. Bamburg and grants from the Japanese Ministry of Education, Science, and Culture to T. Obinata and H. Abe.

Received for publication 8 May 1995 and in revised form 21 December 1995.

References

Abe, H., T. Endo, K.Yamamoto, and T. Obinata. 1990. Sequence of cDNAs encoding actin depolymerizing factor and cofilin of embryonic chicken skeletal muscle: two functionally distinct actin-regulatory proteins exhibit high structural homology. *Biochemistry.* 29:7420–7425.

Adams, M.E., L.S. Minamide, G. Duester, and J.R. Bamburg. 1990. Nucleotide sequence and expression of a cDNA encoding chick brain actin depolymerizing factor. *Biochemistry.* 29:7414–7420.

Agnew, B.J., L.S. Minamide, and J.R. Bamburg. 1995. Reactivation of phosphorylated actin depolymerizing factor and identification of the regulatory site. *J. Biol. Chem.* 270:17582–17587.

Bamburg, J.R., and D. Bray. 1987. Distribution and cellular localization of actin depolymerizing factor. *J. Cell Biol.* 105:2817–2825.

Bamburg, J.R., and B.W. Bernstein. 1991. Actin and actin-binding proteins in neurons. *In* The Neuronal Cytoskeleton. R.D. Burgoyne, editor. Wiley-Liss, NY. pp. 121–160.

Bamburg, J.R., H.E. Harris, and A.G. Weeds. 1980. Partial purification and characterization of an actin depolymerizing factor from brain. *FEBS Lett.* 121:178–182.

Bamburg, J.R., L.S. Minamide, T.E. Morgan, S.M. Hayden, K.A. Giuliano, and A. Koffer. 1991. Purification and characterization of low molecular weight actin depolymerizing proteins from brain and cultured cells. *Methods Enzymol.* 196:125–140.

Baorto, D.M., W. Mellado, and M.L. Shelanski. 1992. Astrocyte process growth induction by actin breakdown. *J. Cell Biol.* 117:357–367.

Bernstein, B.W., and J.R. Bamburg. 1982. Tropomyosin binding to F-actin protects the F-actin from disassembly by brain actin-depolymerizing factor (ADF). *Cell Motil.* 2:1–8.

Bisbee, C.A., M.A. Baker, A.C. Wilson, I. Hadji-Azimi, and M. Fischberg. 1977. Albumin in phylogeny for clawed frogs (*Xenopus*). *Science (Wash. DC).* 195:785–787.

Blin, N., and D.W. Stafford. 1976. A general method for isolation of high molecular weight DNA from eukaryotes. *Nucleic Acids Res.* 3:2303–2308.

Chalfie, M., Y. Tu, G. Euskirchen, W.W. Ward, and D.C. Prasher. 1994. Green fluorescent protein as a marker for gene expression. *Science (Wash. DC).* 263:802–805.

Chomczynski, P., and N. Sacchi. 1987. Single-step method of RNA isolation by acid guanidinium thiocyanate-phenol-chloroform extraction. *Anal. Biochem.* 162:156–159.

Davidson, M.M.L., and R.J. Haslam. 1994. Dephosphorylation of cofilin in stimulated platelets: role for a GTP-binding protein and Ca^{2+}. *Biochem. J.* 301:41–47.

Edwards, K.A., R.A. Montague, S. Shepard, B.A. Edgar, R.L. Erikson, and D.P. Kiehart. 1994. Identification of *Drosophila* cytoskeletal proteins by induction of abnormal cell shape in fission yeast. *Proc. Natl. Acad. Sci. USA.* 91:4589–4593.

Fishkind, D.J., and Y.-L. Wang. 1995. New horizons for cytokinesis. *Curr. Opin. Cell Biol.* 7:23–31.

Furuse, M., T. Hirase, M. Itoh, A. Nagafuchi, S. Yonemura, S. Tsukita, and S. Tsukita. 1993. Occludin: a novel integral membrane protein localizing at tight junctions. *J. Cell Biol.* 123:1777–1788.

Gill, S.C., and P.H. von Hippel. 1989. Calculation of protein extinction coefficients from amino acid sequence data. *Anal. Biochem.* 182:319–326.

Gunsalus, K.C., S. Bonaccorsi, E. Williams, F. Verni, M. Gatti, and M.L. Goldberg. 1995. Mutations in twinstar, a *Drosophila* gene encoding a cofilin/ADF homologue, result in defects in centrosome migration and cytokinesis. *J. Cell Biol.* 131:1243–1259.

Harland, R.M. 1991. *In situ* hybridization: an improved whole-mount method for *Xenopus* embryos. *In* Methods Cell Biology. B.K. Kay and H.B. Peng, editors. Academic Press, San Diego, CA. Vol. 36. pp. 685–694.

Harris, H.E., J.R. Bamburg, B.W. Bernstein, and A.G. Weeds. 1982. The depolymerization of actin by specific proteins from plasma and brain: a quantitative assay. *Anal. Biochem.* 119:102–114.

Hawkins, M., B. Pope, S.K. Maciver, and A.G. Weeds. 1993. The interaction of human actin depolymerizing factor with actin is pH regulated. *Biochemistry.* 32:9985–9993.

Hayden, S.M., P.S. Miller, A. Brauweiler, and J.R. Bamburg. 1993. Analysis of the interactions of actin depolymerizing factor with G- and F-actin. *Biochemistry.* 32:9994–10004.

Iida, K., and I. Yahara. 1986. Reversible induction of actin rods in mouse C3H-2K cells by incubation in salt buffers and treatment with non-ionic detergents. *Exp. Cell Res.* 164:492–506.

Iida, K., K. Moriyama, S. Matsumoto, H. Kawasaki, E. Nishida, and H. Sakai. 1993. Isolation of a yeast essential gene, COF1, that encodes a homologue of mammalian cofilin, a low-M_r actin binding and depolymerizing protein. *Gene (Amst.).* 124:115–120.

Johnson, G.D., and G.M. de C. Nogueira Araujo. 1981. A simple method for reducing the fading of immunofluorescence during microscopy. *J. Immunol. Methods.* 43:349–350.

Kay, B.K., and B.H. Peng. 1991. *Xenopus laevis*: practical uses in cell and molecular biology. *Methods Cell Biol.* 694 pp.

Kohler, G., M. Schrier, H. Hengart, T. Staehlin, J. Stocker, and B. Takass. 1980. Hybridoma Techniques. Cold Spring Harbor Laboratory, Cold Spring Harbor, NY.

Laemmli, U.K. 1970. Cleavage of structural proteins during the assembly of the head of bacteriophage T4. *Nature (Lond.).* 227:680–684.

Léna, J.Y., J.R. Bamburg, A. Rabié, and C. Faivre-Sarrailh. 1991. Actin depolymerizing factor (ADF) in the cerebellum of the developing rat: a quantitative immunocytochemical study. *J. Neurosci. Res.* 30:18–27.

Manes, M.E., R.P. Elinson, and F.D. Barbieri. 1978. Formation of the amphibian grey crescent: effects of colchicine and cytochalasin B. *Roux Arch.* 185: 99–104.

McKim, K.S., C. Matheson, M.A. Marra, M.F. Wakarchuk, and D.L. Baillie. 1994. The *Caenorhabditis elegans* unc-60 gene encodes proteins homologous to a family of actin-binding proteins. *Mol. Gen. Genet.* 242:346–357.

Minamide, L.S., and J.R. Bamburg. 1990. A sensitive dye-binding filter paper assay for the quantitative determination of protein in the presence of reducing agents and detergents. *Anal. Biochem.* 190:66–70.

Moon, A., and D.G. Drubin. 1995. The ADF/cofilin proteins. Stimulus-responsive modulators of actin dynamics. *Mol. Biol. Cell.* 6:1423–1431.

Moon, A.L., P. Janmey, K.A. Louie, and D. Drubin. 1993. Cofilin is an essential component of the yeast cortical cytoskeleton. *J. Cell Biol.* 120:421–435.

Morgan, T.E., R.O. Lockerbie, L.S. Minamide, M.D. Browning, and J.R. Bamburg. 1993. Isolation and characterization of a regulated form of actin depolymerizing factor. *J. Cell Biol.* 122:623–633.

Moriyama, K., K. Iida, and I. Yahara. 1996. Phosphorylation of ser-3 of cofilin regulates its essential function on actin. *Genes to Cells.* In press.

Mullholland, J., D. Preuss, A. Moon, A. Wong, D. Drubin, and D. Botstein. 1994. Ultrastructure of the yeast actin cytoskeleton and its association with the plasma membrane. *J. Cell Biol.* 125: 381–391.

Nagaoka, R., H. Abe, K. Kusano, and T. Obinata. 1995. Concentration of cofi-

lin, a small actin-binding protein, at the cleavage furrow during cytokinesis. *Cell Motil. Cytoskeleton.* 30:1–7.

Nieuwkoop, P.D., and J. Faber. 1967. Normal table of *Xenopus laevis* (Daudin): a systematic chronological survey of the development of the fertilized egg till the end of metamorphosis. 2nd edition. Elsevier Science/North-Holland, Amsterdam.

Nishida, E., S. Maekawa, and H. Sakai. 1984. Cofilin, a protein in porcine brain that binds to actin filaments and inhibits their interactions with myosin and tropomyosin. *Biochemistry.* 23:5307–5313.

O'Farrell, P.H. 1975. High resolution two-dimensional electrophoresis of proteins. *J. Biol. Chem.* 250:4007–4021.

O'Farrell, P.Z., H.M. Goodman, and P.H. O'Farrell. 1977. High resolution two-dimensional electrophoresis of basic as well as acidic proteins. *Cell.* 12:1133–1141.

Ohta, Y., E. Nishida, H. Sakai, and E. Miyamoto. 1989. Dephosphorylation of cofilin accompanies heat shock-induced nuclear accumulation of cofilin. *J. Biol. Chem.* 264:16143–16148.

Ono, S., N. Minami, H. Abe, and T. Obinata. 1994. Characterization of a novel cofilin isoform that is predominantly expressed in mammalian skeletal muscle. *J. Biol. Chem.* 269:15280–15286.

Pollard, T.D., and J.A. Cooper. 1986. Actin and actin-binding proteins. A critical evaluation of mechanisms and functions. *Annu. Rev. Biochem.* 55:987–1035.

Rosenblatt, J., P. Peluso, and T.J. Mitchison. 1995. The bulk of unpolymerized actin in Xenopus egg extracts is ATP-bound. *Mol. Biol. Cell.* 6:227–236.

Saito, T., F. Lamy, P.P. Roger, R. Leqocq, and J. Dumont. 1994. Characterization and identification as cofilin and destrin of two thyrotropin- and phorbol ester-regulated phosphoproteins in thyroid cells. *Exp. Cell Res.* 212:49–61.

Samstag, Y., C. Eckerskorn, S. Wesselborg, S. Henning, R. Wallach, and S.C. Meuer. 1994. Costimulatory signals for human T-cell activation induce nuclear translocation of pp19/cofilin. *Proc. Natl. Acad. Sci. USA.* 91:4494–4498.

Sanger, F., S. Nicklen, and A.R. Coulson. 1977. DNA sequencing with chain terminating inhibitors. *Proc. Natl. Acad. Sci. USA.* 74:5463–5467.

Singal, P.K., and E.J. Sanders. 1974. An ultrastructural study of the first cleavage of *Xenopus laevis*. *J. Ultrastruct. Res.* 47:433–451.

Stossel, T.P. 1993. On the crawling of animal cells. *Science (Wash. DC.).* 260: 1086–1094.

Studier, F.W., A.H. Rosenberg, J.J. Dunn, and J.W. Dubendorff. 1990. Use of T7 RNA polymerase to direct expression of cloned genes. *Methods Enzymol.* 185:60–89.

Sun, H.-Q., K. Kwiatkowska, and H.L. Yin. 1995. Actin monomer binding proteins. *Curr. Opin. Cell Biol.* 7:102–110.

Suzuki, K., T. Yamaguchi, T. Tanaka, T. Kawanishi, T. Nishimaki-Mogami, K. Yamamoto, T. Tsuji, T. Irimura, T. Hayakawa, and A. Takahashi. 1995. Activation induces dephosphorylation of cofilin and its translocation to plasma membranes in neutrophil-like differentiated HL-60 cells. *J. Biol.Chem.* 270: 19551–19556.

Vincent, J.-P., and J.C. Gerhart. 1987. Subcortical rotation in *Xenopus* eggs: an early step in embryonic axis specification. *Dev. Biol.* 123:526–539.

Vincent, J.-P., G.F. Oster, and J.C. Gerhart. 1986. Kinematics of gray crescent formation in *Xenopus* eggs: the displacement of subcortical cytoplasm relative to the egg surface. *Dev. Biol.* 113:484–500.

Wessel, D., and U.I. Flügge. 1984. A method for the quantitative recovery of protein in dilute solution in the presence of detergents and lipids. *Anal. Biochem.* 138:141–143.

Yamamoto, M., T. Yamagishi, H. Yaginuma, K. Murakami, and N. Ueno. 1994. Localization of thymosin b4 to the neural tissues during the development of *Xenopus laevis*, as studied by in situ hybridization and immunocytochemistry. *Dev. Brain Res.* 79:177–185.

Yonezawa, N., E. Nishida, and H. Sakai. 1985. pH-Control of actin polymerization by cofilin. *J. Biol. Chem.* 27:14410–14412.

Yonezawa, N., E. Nishida, S. Koyasu, S. Maekawa, Y. Ohta, I. Yahara, and H. Sakai. 1987. Distribution among tissues and intracellular localization of cofilin, a 21 kD actin-binding protein. *Cell Struct. Funct.* 2:443–452.